Supplemental Information for Variable Surface Transport Modalities on Functionalized Nylon Films Revealed with Single Molecule Spectroscopy

Authors: Lawrence J. Tauzin†, Hao Shen†, Cathy A. Bothof, George W. Griesgraber, Amy K. McNulty, Jerald K. Rasmussen ‡, Christy F. Landes*†

† Department of Chemistry, Rice University, Houston, Texas 77251, United States

‡ 3M Corporate Research Laboratories, 3M Center 201-3E-03, St. Paul, MN 55144

Contents

Nylon Film Thickness

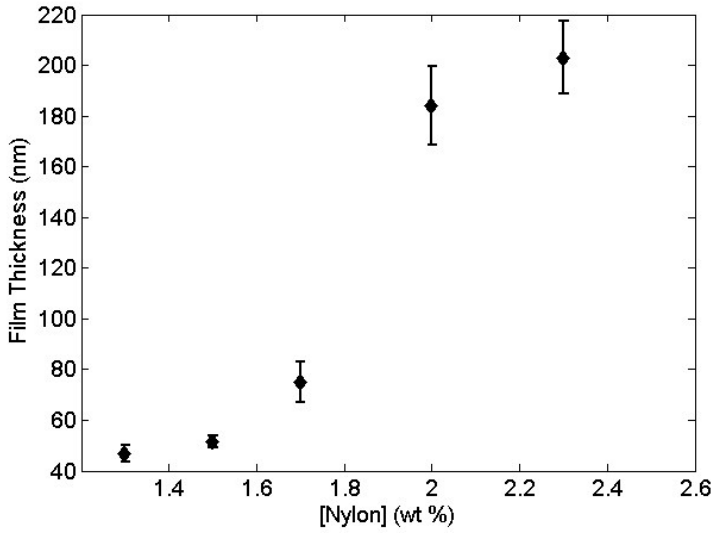

Figure S1. Film thickness vs. nylon solution concentration. Concentration given as wt % in formic acid. Error bars represent the standard deviation calculated from 10 thickness measurements at different regions of the film.

AFM Characterization

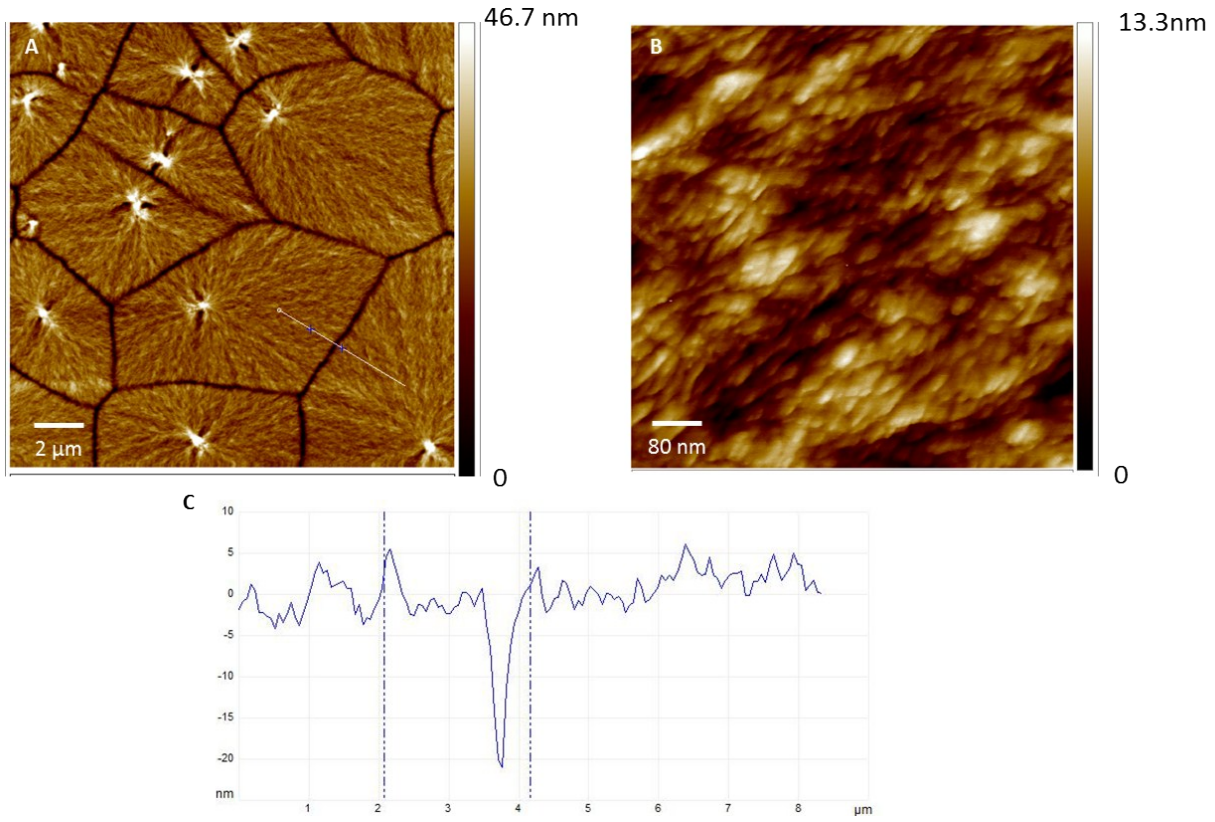

Figure S2. AFM characterization of unfunctionalized nylon 6,6 films. (A) 25 x 25 µm AFM height image, (B) 1 x 1 µm AFM height image. (C) Line section of the line shown in (A). The rms surface roughness was calculated to be 0.46 nm.

Ligand Synthesis

4-Aminobutyric acid/VDM Monomer Synthesis

4-Aminobutyric acid (Alfa Aesar, 15.45 grams, 0.15 mole) wss charged into a 500 mL round bottomed flask. A magnetic stir bar was added, followed by 1.00 N sodium hydroxide solution (J.T. Baker, 150 mL). The flask was immersed in an ice-water bath and the mixture was stirred magnetically for 20 minutes. At this time, 2-vinyl-4,4-dimethylazlactone (VDM, SNPE,

Inc., 10 mL) was added by syringe. Stirring was continued for 5 to 10 minutes, or until the mixture appeared to be homogeneous. Then an additional charge of VDM (9.2 mL, total of 0.15 mole) was added. Stirring was continued as the bath was allowed to warm to room temperature (about 2 hours total reaction time). ^{1}H-NMR analysis indicated clean conversion to the desired monomer. The pH of the mixture was adjusted to pH 7.0 by addition of a few drops of concentrated hydrochloric acid. The final solution was approximately 20.95% solids as measured by Ohaus moisture balance.

^{1}H-NMR (500 MHz, D_2O) δ 1.34 (s, 6H), 1.59 (p, 2H), 2.04 (t, 2H), 3.05 (t, 2H), 5.62 (d, 1H), 6.0-6.2 (m, 2H).

2-Isocyanatoethyl methacrylate/Agmatine Monomer Synthesis

Agmatine sulfate (Sigma Aldrich, 100 g, 0.397 mol) was dissolved in 400 mL of aqueous 1.00 N NaOH. Acetone (200 mL) was then added and the stirred mixture was cooled to about 10 °C in a cold water bath. An additional 80 mL of H_2O was added to keep the agmatine sulfate in solution. 2-isocyanatoethyl methacrylate (Showa Denko, 58.0 mL, 0.411 mol) was then added to the reaction mixture, via an addition funnel, over a period of 30 min. After stirring an additional 45 min, the reaction mixture was placed on a rotary evaporator at ambient temperature. After pulling off most of the acetone, the reaction mixture was transferred to a separatory funnel and washed with ethyl acetate (2 x 250 mL) and methylene chloride (2 x 200 mL). The remaining aqueous solution was adjusted to pH 7 by addition of a small amount of dilute sulfuric acid and then placed on a rotary evaporator at ambient temperature to draw off any remaining volatiles. Lyophilization yielded the title compound (162 g) as a white powder.

^{1}H-NMR (500 MHz, D_2O) □ 1.22 (s, 3H), 1.61-1.48 (m, 4H), 3.12 (t, J = 6.4 Hz, 2H), 3.18 (t, J = 7.0 Hz, 2H), 3.45 (t, J = 5.4 Hz, 2H), 4.23 (t, J = 5.2 Hz, 2H), 5.73 (s, 1H), 6.14 (s, 1H).

Single Particle Tracking

Data analysis was conducted using custom algorithms written in Matlab R2011b. The raw data from the EMCCD detector was analyzed as a series of 2 dimensional images. Details on the particle identification method have been published elsewhere.[1] Our program first increases the signal to noise ratio (SNR) of each frame by convolution between the frame and a 3 × 3 matrix of ones. This will increase the SNR by 2 to 3 times. Then the program calculates the local background and local noise level. The corresponding local intensity threshold equals to local background plus three times standard deviation of local noise. Particles are pre-identified as pixels having local maximum intensities. The local maximum intensity is compared within an input distance. We used a distance of three pixels for all our analysis. After that, the centers of all the pre-identified particles are calculated using radial symmetry algorithm. The second moment of the particle is compared with the second moment of the same fitting region with Gaussian noise. Only if the second moment of the particle is smaller than the 90 % of the second momentum of Gaussian noise, we will consider this particle as a real particle and record its positions. Finally, we used nearest distance algorithm combining with local optimum to generate the trajectories. More details about the program are explained in ref 1.

Radius of Gyration Evolution Analysis

Radius of gyration can be used to quantify the area explored by a tracked molecule. This technique has been used previously to study systems displaying intermittent surface interaction.[2]

The radius of gyration of a particle (R_g) is calculated at each point in the trajectory using the following equation:

$$R_g = \sqrt{R_1 + R_2} \tag{2}$$

where R_1 and R_2 correspond to the major and minor eigenvalues of the radius of gyration tensor T. The tensor corresponds to the two by two matrix:

$$T = \begin{pmatrix} \frac{1}{N}\sum_{i=1}^{N}(x_i - \langle x\rangle)^2 & \frac{1}{N}\sum_{i=1}^{N}(x_i - \langle x\rangle)(y_i - \langle y\rangle) \\ \frac{1}{N}\sum_{i=1}^{N}(x_i - \langle x\rangle)(y_i - \langle y\rangle) & \frac{1}{N}\sum_{i=1}^{N}(y_i - \langle y\rangle)^2 \end{pmatrix} \tag{3}$$

where N is the number of steps in the trajectory, x and y are the x and y locations of the particle. The evolution of the radius of gyration with time is established by calculating R_g for each time step in a trajectory. For this work, only the R_g value for the entire trajectory is considered.

α-lactalbumin Adsorption to IEM-Agmatine Functionalized Films Raw Trajectories

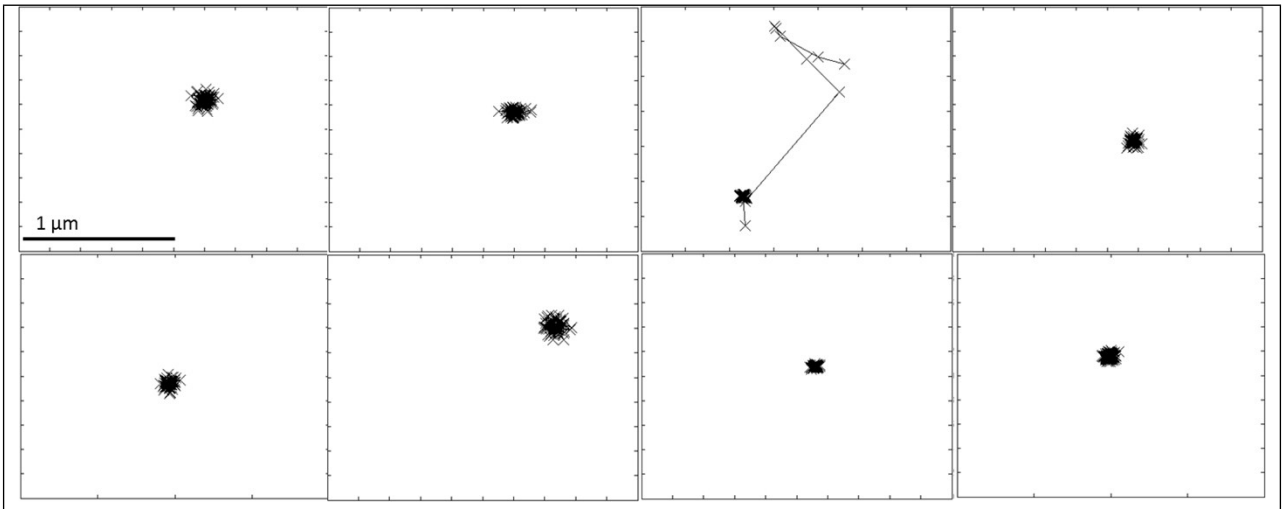

Figure S3. Representative trajectories of α-lactalbumin adsorbing to IEM-Agmatine functionalized nylon 6,6 films (30 minute deposition time).

Lysozyme Adsorption to GABA/VDM Functionalized Films Raw Trajectories

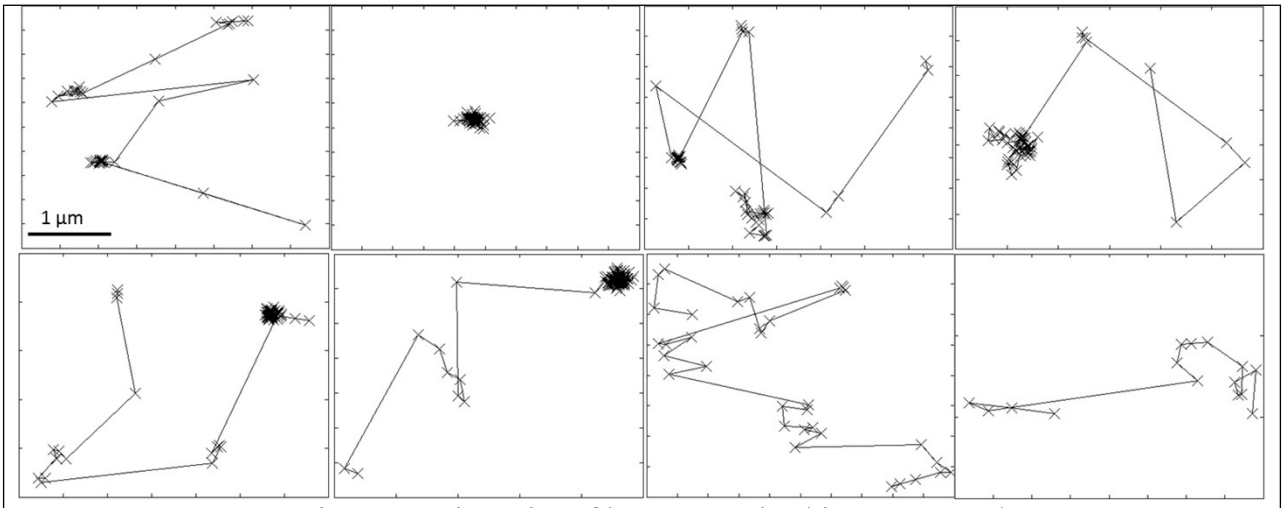

Figure S4. Representative raw trajectories of lysozyme adsorbing to GABA/VDM functionalized nylon 6,6 films (30 minute deposition time).

van Hove Displacement Plots

α-Lactalbumin Adsorption to IEM-Agmatine

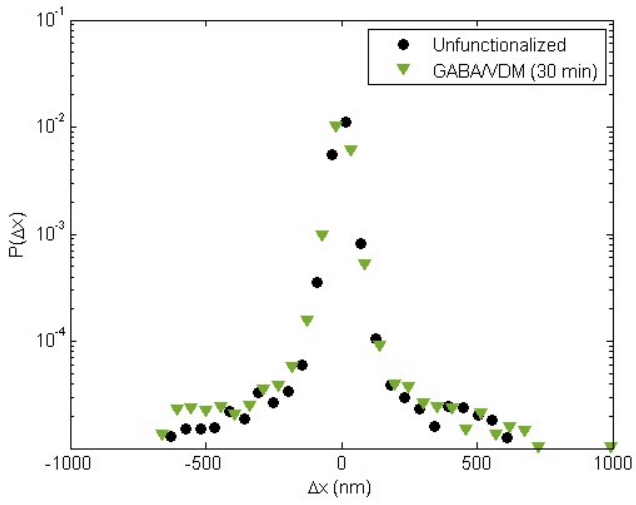

Figure S5. Probability distribution of single frame step sizes for 50 pM α-lactalbumin adsorbing to unfunctionalized and IEM-Agmatine functionalized nylon 6,6. This data is the same as the 0 and 30 minute data shown in figure 3 of the main text.

Lysozyme adsorption to GABA/VDM

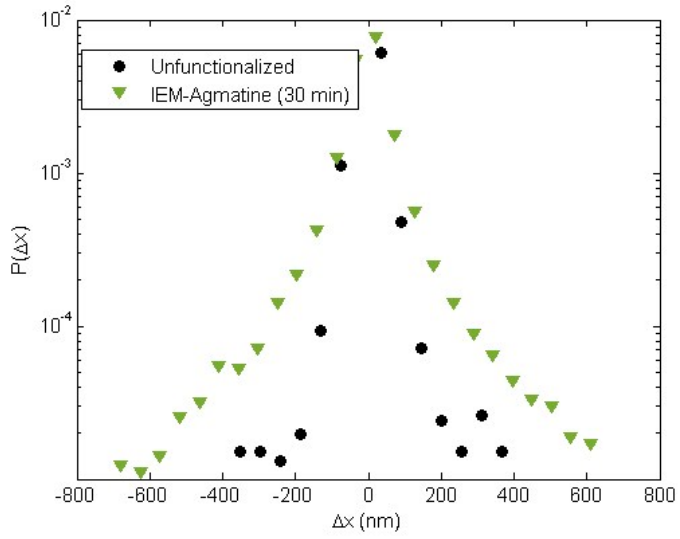

Figure S6. Probability distribution of single frame step sizes for 1 nM lsyzoyme adsorbing to unfunctionalized and GABA/VDM functionalized nylon 6,6. This data is the same as the 0 and 30 minute data shown in figure 2 of the main text.

α-lactalbumin Adsorption to GABA/VDM Functionalized Films

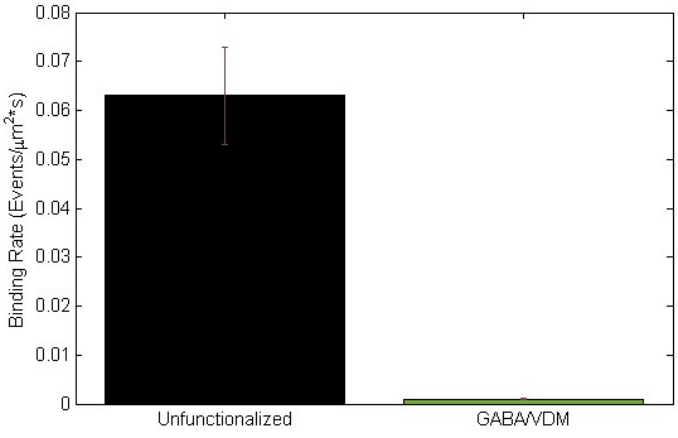

Figure S7. Comparison of 500 pM α-lactalbumin adsorption to unfunctionalized nylon 6,6 and nylon 6,6

functionalized with GABA/VDM (30 minute deposition time).

α-lactalbumin shows reduced binding to GABA/VDM functionalized films most likely due to electrostatic repulsion. The binding rate was so low that an analysis of single frame displacement distributions was not possible due to an insufficient number of trajectories.

Lysozyme Binding to IEM-Agmatine Functionalized Films

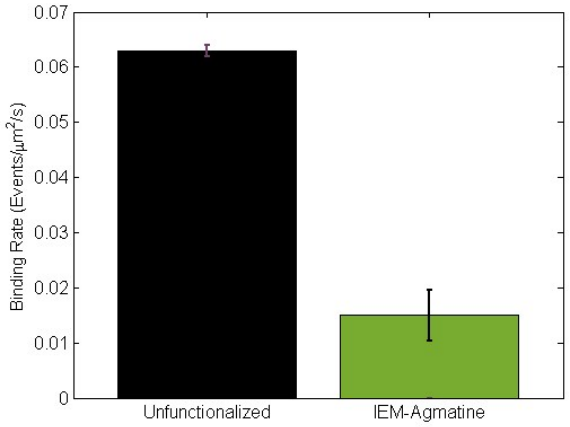

Figure S8. Comparison of 1 nM lysozyme adsorption to unfunctionalized nylon 6,6 and nylon 6,6 functionalized with IEM-Agmatine (30 minute deposition time).

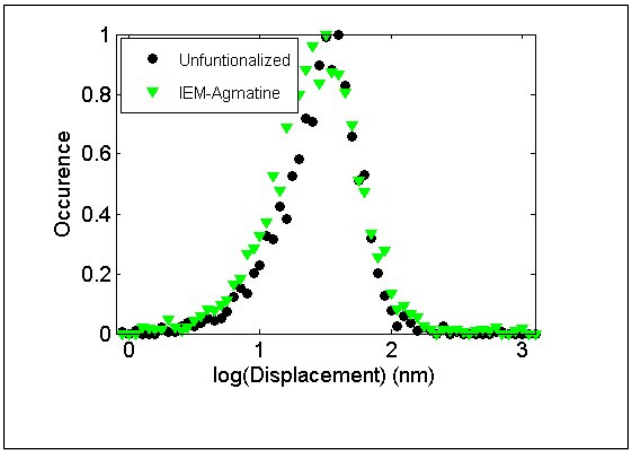

Figure S9. Single frame displacement histograms for lysozyme adsorbing to unfunctionalized and IEM-Agmatine functionalized (30 minute deposition time) nylon films.

Lysozyme also shows reduced adsorption to films functionalized with the like charged IEM-Agmatine. Additionally, no hopping was observed for this protein/ligand combination. These controls suggest that the enhanced surface diffusion through hopping is a property unique to certain protein/ligand combinations.

Surface Diffusion Coefficients of Proteins Adsorbing to Functionalized Nylon Films

Diffusion coefficients were calculated from the trajectories of lysozyme and α-lactalbumin interacting with functionalized nylon films. The calculations were performed using a custom maximum likelihood estimator developed for short single molecule trajectories.[3]

α-lactalbumin Adsorbing to IEM-Agmatine

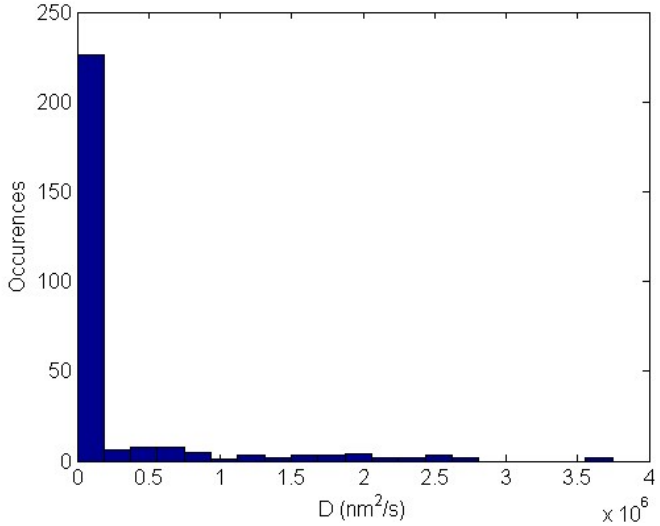

Figure S10. Diffusion coefficient histogram for α-lactalbumin adsorbing to IEM-Agmatine (30 minute deposition time) for 1,000 frames worth of trajectories.

Lysozyme Adsorbing to GABA/VDM

Figure S11. Diffusion coefficient histogram for lysozyme adsorbing to GABA/VDM (30 minute deposition time) for 1,000 frames worth of trajectories.

Surface Dwell Time Curve Fit Parameters

	A1 (%)	τ1 (s)	A2 (%)	τ2 (s)	A3 (%)	τ3 (s)	Avg (s)
GABA/VDM (Unfunctionalized)	2	0.56	7	0.10	91	0.02	0.012
GABA/VDM (Functionalized)	6	0.55	37	0.13	57	0.03	0.03
IEM-Agmatine (Unfunctionalized)	1	1.1	16	0.25	83	0.04	0.03
IEM-Agmatine (Functionalized)	13	0.27	44	0.09	43	0.03	0.03

Table S1. Fit parameters from the surface dwell time curves presented in Figure 4 fit with triple exponential decays. The Avg. column represents the weighted average of the 3 decay times for each curve.

Single Site Dwell Time Curve Fit Parameters

	A1 (%)	τ1 (s)	A2 (%)	τ2 (s)	A3 (%)	τ3 (s)	Avg (s)
GABA/VDM (Unfunctionalized)	9	0.70	5	0.14	86	0.014	0.012
GABA/VDM (Functionalized)	3	0.37	43	0.06	54	0.03	0.02
IEM-Agmatine (Unfunctionalized)	1	1.2	18	0.18	81	0.04	0.03
IEM-Agmatine (Functionalized)	8	0.29	36	0.12	56	0.03	0.02

Table S2. Fit parameters from the surface dwell time curves presented in Figure 4 fit with triple exponential decays. The Avg. column represents the weighted average of the 3 decay times for each curve.

Passivation of Strong Sites with High Protein Concentrations

In order to support the hypothesis that strong binding sites on the nylon surface contribute to the elongated tails of the dwell time distributions, we conducted control experiments with both high (1 μM) and low (50 pM) concentrations of α-lactalbumin. In the high concentration experiments, we add 1 μM unlabeled α-lactalbumin to the probe solution mixture. The unlabeled protein molecules should bind to and effectively passivate strong adsorption sites leading to a lower probability that the labeled probe molecules will bind to them.[4]

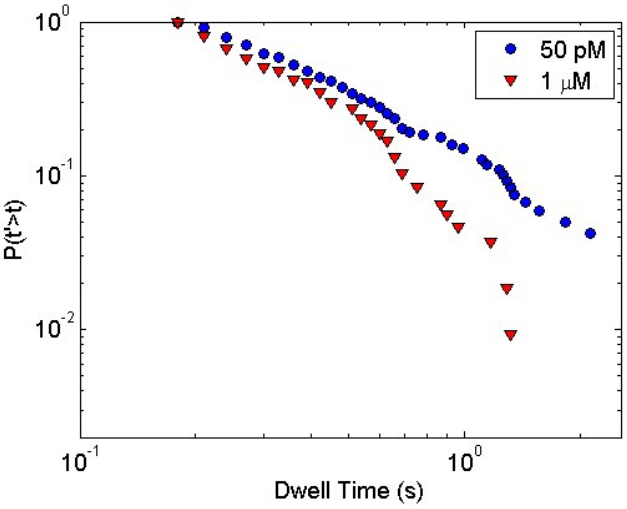

Figure S12. Single site dwell times for high and low concentrations of α-lactalbumin binding to unfunctionalized nylon 6,6.

The distribution is found to decay faster in the presence of 1 μM protein solution which supports the hypothesis that strong sites are present on the unfunctionalized nylon film and that passivation of these sites leads to a faster decay in the observed dwell time distribution.

Protein Surface Charge Distribution

Surface charge distributions were calculated and modeled using the PDB2PQR web server available at http://nbcr-222.ucsd.edu/pdb2pqr_2.0.0/

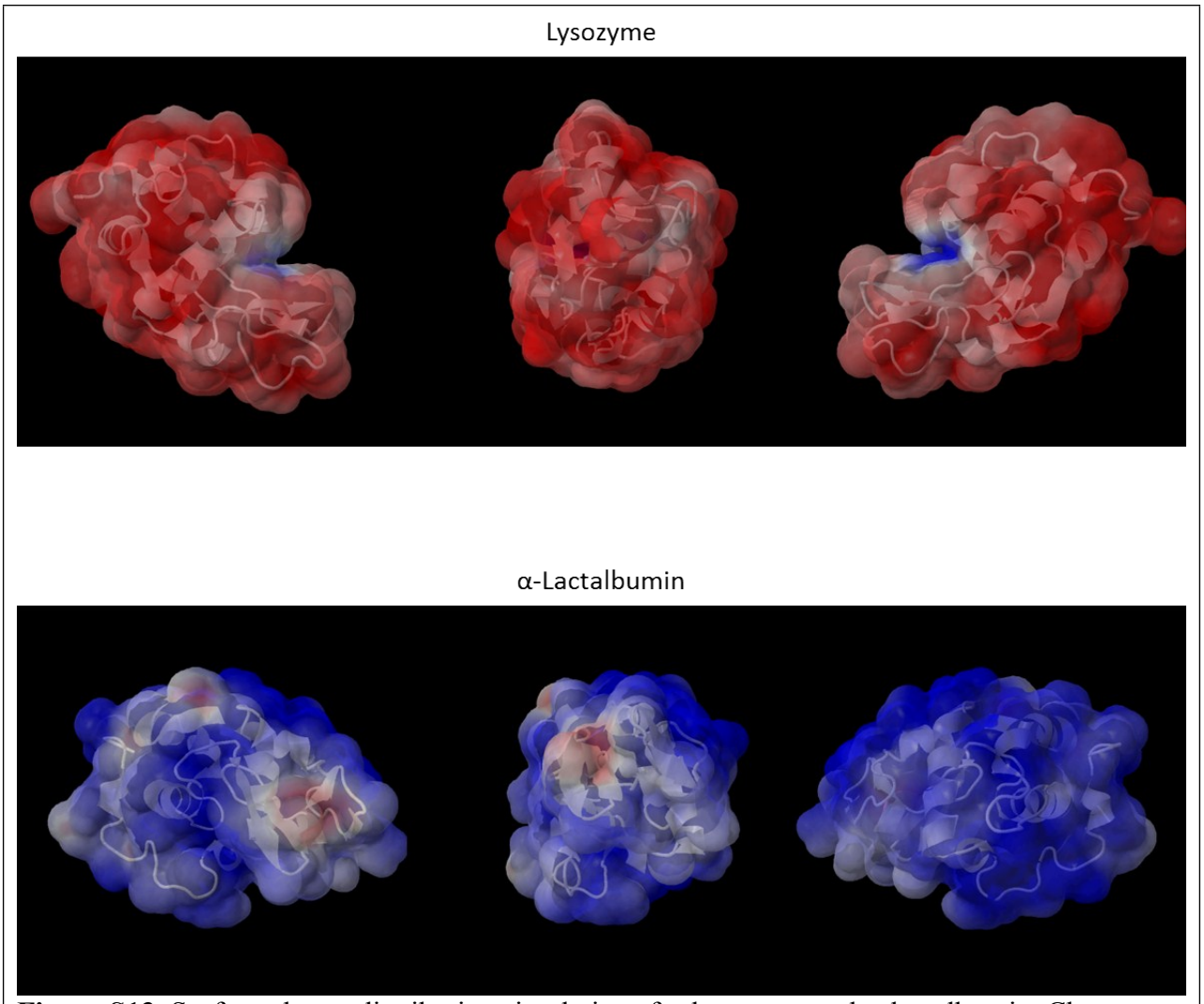

Figure S13. Surface charge distribution simulations for lysozyme and α-lactalbumin. Charge contours shown at -5 kT/e (blue) and +5 kT/e (red)

References

1. Shuang, B.; Chen, J.; Kisley, L.; Landes, C. F., Troika of single particle tracking programing: SNR enhancement, particle identification, and mapping. *Phys. Chem. Chem. Phys.* **2014,** *16* (2), 624-634.
2. Tauzin, L. J.; Shuang, B.; Kisley, L.; Mansur, A. P.; Chen, J.; de Leon, A.; Advincula, R. C.; Landes, C. F., Charge-Dependent Transport Switching of Single Molecular Ions in a Weak Polyelectrolyte Multilayer. *Langmuir* **2014,** *30* (28), 8391-8399.
3. Shuang, B.; Byers, C. P.; Kisley, L.; Wang, L.-Y.; Zhao, J.; Morimura, H.; Link, S.; Landes, C. F., Improved analysis for determining diffusion coefficients from short, single-molecule trajectories with photoblinking. *Langmuir* **2012,** *29* (1), 228-234.
4. Langdon, B. B.; Mirhossaini, R. B.; Mabry, J. N.; Sriram, I.; Lajmi, A.; Zhang, Y.; Rojas, O. J.; Schwartz, D. K., Single-Molecule Resolution of Protein Dynamics on Polymeric Membrane Surfaces: The Roles of Spatial and Population Heterogeneity. *ACS Appl. Mater. Interfaces* **2015,** *7* (6), 3607-3617.